Talanta 83 (2010) 404–409

Contents lists available at ScienceDirect

Talanta

journal homepage: www.elsevier.com/locate/talanta

Linear and non linear chemometric models to quantify the adulteration of extra virgin olive oil

José S. Torrecilla*, Ester Rojo, Juan C. Domínguez, Francisco Rodríguez

Department of Chemical Engineering, Faculty of Chemistry, University Complutense of Madrid, 28040 Madrid, Spain

ARTICLE INFO

Article history:
Received 11 June 2010
Received in revised form 26 August 2010
Accepted 25 September 2010

Keywords:
Chaos
Fractal dimension
Lyapunov exponent
Autocorrelation function
UV–vis
Adulteration
Olive oils
Sunflower oil
Corn oil

ABSTRACT

Two mathematical methods to quantify adulterations of extra virgin olive oil (EVOO) with refined olive oil (ROO), refined olive-pomace oil (ROPO), sunflower (SO) or corn (CO) oils have been described here. These methods are linear and non linear models based on chaotic parameters (CPs, Lyapunov exponent, autocorrelation coefficients and two fractal dimensions) which were calculated from UV–vis scans (190–900 nm wavelength) of 817 adulterated EVOO samples. By an external validation process, linear and non linear integrated CPs/UV–vis models estimate concentrations of adulterant agents with a mean correlation coefficient (estimated *versus* real concentration of cheaper oil) greater than 0.80 and 0.97 and a mean square error less than 1% and 0.007%, respectively. In the light of the results shown in this paper, the adulteration of EVOO with ROO, ROPO, SO and CO can be suitably detected by only one chaotic parameter integrated on a radial basis network model.

1. Introduction

For centuries, the adulteration of food products with cheaper and more readily available substitutes has been a worldwide problem. Currently, adulteration of foods is more and more prevalent, mainly in those products with relatively high prices such as extra virgin olive oil (EVOO). Due to this, a large number of cases of adulteration of oily juice have been detected recently. The substitution or adulteration of EVOO with cheaper ingredients is not only economic fraud, but may also on occasion have severe health implications for consumers. An example being the Spanish toxic oil syndrome resulting from the consumption of aniline denaturalized rapeseed oil that involved more than twenty thousand people, causing serious illness and even death [1–3].

To fight against the increase in these fraudulent activities two measures are being taken. The chemical compositions of specific olive oils have been qualified and protected by certificates of protected designation of origin issued by a government body. Analytical techniques, physicochemical parameters, indexes, etc. [4–6] and their integration with mathematical algorithms [7,8] have also been proposed. In the latter group, several techniques based on chemometric tools and analytical techniques have been developed to authenticate and detect olive oil adulteration. One good example is the chromatographic techniques, including gas chromatography (GC) [9–11], gas chromatography–mass spectrometry [12–14], high-performance liquid chromatography [15–17]. Other examples are nuclear magnetic resonance spectroscopy [18–20] or Fourier transformed infrared spectroscopic method [21]. The combination of the aforementioned techniques and DSC has also been used to carry out quality control and detect the adulteration of edible oils [22–24]. Although these methods are widely used to detect low concentrations of adulterating agents, they require complicated and expensive laboratory facilities. In addition, given that their sampling times are habitually higher than the sample preparation time, these techniques cannot be applied to control on-line the quality of the EVOO during the manufacturing process. Considering these important requirements and the associated risks of adulteration of foods, the development of a simple, cheap, and rapid alternative to detect the adulterating agent in EVOO is necessary.

Regretfully, the ideal tool for the detection of minute concentration of every possible adulterant product is not reality. Nevertheless, currently, chemometric tools based on partial least squares [25], principal component analysis [9], neural networks [7,8], or even chaotic parameters present the most successful and promising results [26].

Recently, it has been more apparent that most chaotic regions can represent dynamical systems, and as they are tools, based on chaotic parameters (CPs), they can detect slight variations in initial

* Corresponding author. Tel.: +34 91 394 42 40; fax: +34 91 394 42 43.
E-mail address: jstorre@quim.ucm.es (J.S. Torrecilla).

0039-9140/$ – see front matter © 2010 Elsevier B.V. All rights reserved.
doi:10.1016/j.talanta.2010.09.048

Table 1
Type of edible oils used to adulterate the extra virgin olive oil samples provided by Aceites Borges Pont SAU (2008–2009 harvest season), brand and number of adulterated oil samples used in the learning, verification and validation samples.

Type of adulterated oils	Number of samples	Brand
Refined olive oil	205	KOIPE, SOS Cuétara SA
Refined olive-pomace oil	204	Aceites Pina SA
Sunflower oil	204	KOIPE, SOS Cuétara SA
Corn oil	204	KOIPE, SOS Cuétara SA

experimental conditions [27–29]. Models based on CPs could be suitable to determine trace chemicals in real samples. Nevertheless, in the chemical field, these types of chaotic models have been described in few manuscripts [27,30]. Although to the best of our knowledge, in the oleic field, there is only one publication where models based on chaotic parameters are shown [26]. The successful results achieved here and in other scientific fields lead us to think that a model based on chaotic parameters would be appropriate to quantify the adulteration of foods. For this reason, the adulteration of commercial EVOO with refined olive oil (ROO) or refined olive-pomace oil (ROPO), sunflower (SO) or corn (CO) oils has been studied here using linear models based on chaotic parameters and a radial basis network model (RBN) based on a fractal dimension (*vide infra*) of UV–vis scans of adulterated EVOO samples. Taking into account that an analytical technique which presents a sampling preparation time less than the process sampling time is required, the UV–vis spectroscopy technique has been applied here. To sum up, a simple and rapid analytical technique, but which is insufficient for the determination of chemicals in real samples, combined with a powerful chemometric tool to correct this lack and create a suitable tool to detect adulterant agents in EVOO.

2. Materials and methods

2.1. Instrumentation and oil samples

A Varian Cary 1E UV–vis spectrophotometer was employed for absorbance measurements from 190 to 900 nm using quartz cells of 1 cm path length. In the determination of absorbance, the expanded uncertainty in the experimental measurement has been found to be less than 0.03. All stock solutions were prepared using an AG 245 Mettler Toledo analytical balance (precision 0.01 mg).

The botanical origin and quality of all samples of extra virgin olive oil were guaranteed by the suppliers (Table 1). The EVOO samples used here came from the same oil producer and corresponded to the 2008–2009 harvest season. In addition, samples of ROO, ROPO, SO and CO have been provided by Spanish companies, which are shown in Table 1. All were stored in the dark at room temperature until the time of analysis which was prior to their date of expiry. To estimate and detect the adulteration of EVOO with other low cost oils, binary mixtures containing EVOO and ROO, ROPO, SO or CO were prepared. Following the procedure shown in the Official Journal of the European Union (Commission Regulation (EC) No. 640/2008, Annex IX), all samples were prepared and diluted in isooctane ($C_8H_{18} \geq 99.5\%$ purity, from MERCK).

2.2. Chaotic parameters used

To detect low grade oils (ROO, ROPO, SO and CO) in the EVOO, several chaotic parameters (Lyapunov exponent, autocorrelation functions and fractal dimensions) have been calculated from UV–vis scans of adulterated EVOO samples.

Lyapunov exponent (LE) provides additional useful information about the system studied [28]. This can be used to measure the sensitivity of a system's behavior under initial conditions. LE also characterizes the dynamic of a complex process, quantifies the average growth of infinitesimally small errors at initial points and describes the rate of separation of infinitesimally close trajectories. The Lyapunov exponent is defined by Eq. (1) [31].

Table 2
Meanings of maximum Lyapunov exponent (MLE) [16].

MLE < 0	Stable fixed
MLE = 0	Stable limit cycle
MLE = ∞	Noise
0 < MLE < ∞	Chaos

$$\text{Lyapunove exponent} = \frac{\sum_{k=1}^{m} \log_2 L(\lambda_k)/L(\lambda_{k-1})}{\Delta\lambda_m} \quad (1)$$

where $\Delta\lambda_m$, k and $L(\lambda_k)$ are the prediction wavelength intervals, the wavelength and the Euclidean distance between the developed points in the space, respectively. For instance, considering p_1 at (λ_{k-1}, Absorbance$_{k-1}$) and p_2 at (λ_k, Absorbance$_k$), the Euclidean distance between p_1 and p_2 ($L(\lambda_{k-1})$) is $\sqrt{(\lambda_{k-1}-\lambda_k)^2 + (\text{Absorbance}_{k-1} - \text{Absorbance}_k)^2}$ (Fig. 1) This parameter is one of the most sensitive to determine the chaotic dynamic of processes [28]. Depending on the sign of the maximal LE (MLE), different types of attractors (dynamical systems evolve after a long period of time) can be found (Table 2). A positive value of the maximal Lyapunov exponent means chaos, that is, the neighbouring points of trajectories in the space diverge [32].

Autocorrelation functions ($R_{\Delta\lambda}$). These parameters measure linearly how strongly, on average, each data point is correlated with wavelength lag ($\Delta\lambda$). These are the ratio of the autocovariance to the variance of the data. In general, $R_{\Delta\lambda}$ is between 1 (small $\Delta\lambda$) and 0 (large $\Delta\lambda$) [28]. $R_{\Delta\lambda}$ is defined by the following equation [32]:

$$R_{\Delta\lambda} = \frac{\sum_{n=1}^{N-k}(X_n - \bar{X})(X_{n-k} - \bar{X})}{\sqrt[z]{\sum_{n=1}^{N-k}(X_n - \bar{X})\sum_{n=1}^{N-k}(X_{n-k} - \bar{X})}} \quad (2)$$

where X, $\bar{X}$ and N represent the absorbance set of the measurements by UV–vis spectrophotometer, their average and the total number of datasets, respectively. Given that the $\Delta\lambda$ value ranges between 0 and 650 wavelength with $\Delta\lambda = 50$, 14 parameters have been calculated. For instance, in the case of $\Delta\lambda = 50$ or $\Delta\lambda = 150$, throughout the work $R_{\Delta\lambda}$ have been referred to as R_{50} or R_{150}, respectively.

Fractal dimensions. One of the most descriptive definitions of fractal is "*A fractal is a subset of R^n which is self-similar and whose fractal dimension exceeds its topological dimension*" [29]. Apparently, there are no relations between dynamic systems and fractal geometry. In classical geometry, the dimension of a line is one, and the square and volume are two and three, respectively, but what is the dimension of the Koch curve or Sierpinski triangle? It is certain that fractal images do not fit into the aforementioned notions of geometrical dimensions. In the Sierpinski triangle, the fractal dimension can be calculated by Eq. (3). This triangle can be subdivided into three triangles ($P = 3$) and can be magnified by a factor (M) of two. With these considerations, the dimension of Sierpinski triangle is equal to 1.584 [29].

$$\text{Fractal dimension} = \frac{\log(P)}{\log(M)} \quad (3)$$

The problem becomes more complex when the fractal dimension of experimental curves is required. In these cases, the fractal dimensions are numbers that quantitatively describe how an object fills its space. This dimension can be calculated by the slope between the number of circles ($N(d)$) necessary to fill an experimental curve and their diameters (d) (Fig. 2). In plane geometry, objects are solid and continuous and given that they have no holes, they have integer dimensions. Fractals are rough and often discontinuous, and so, they present non integer dimensions (*vide infra*). From a frac-

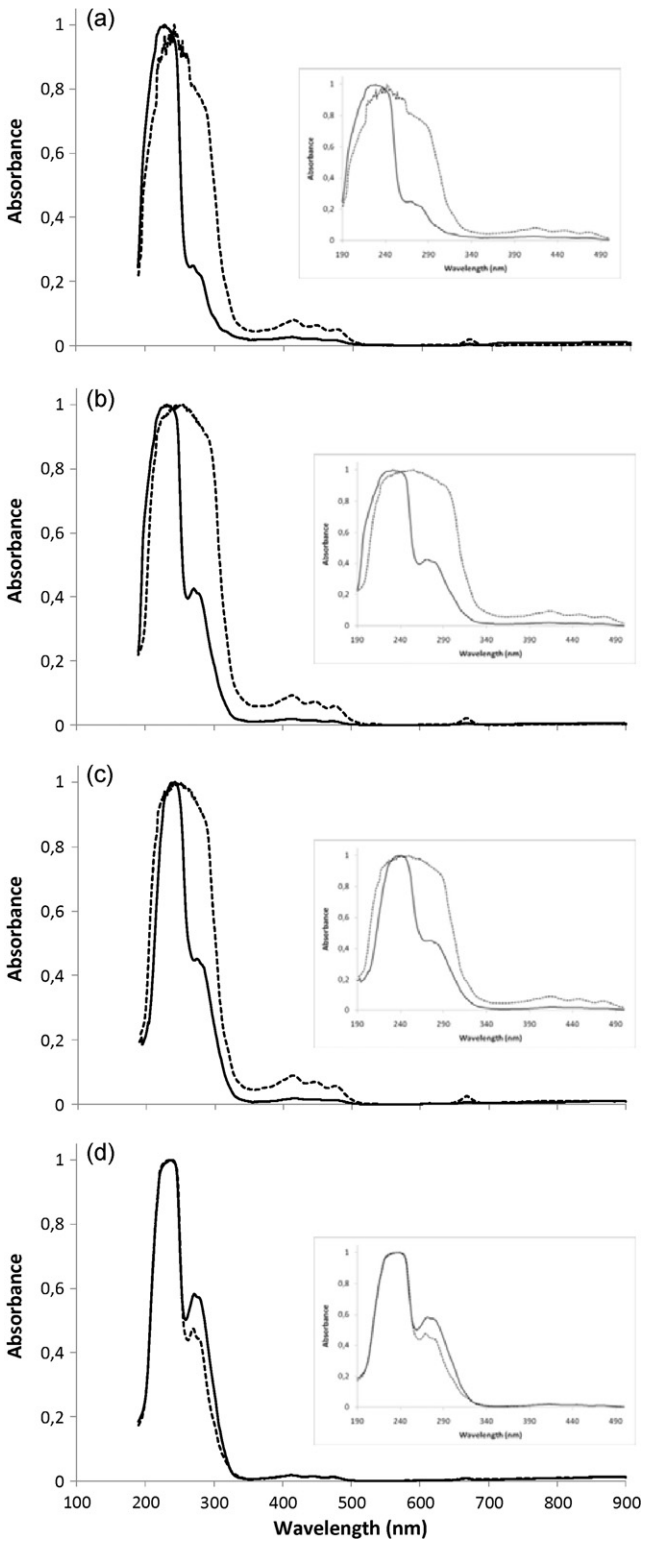

Fig. 1. UV–vis scans of binary mixtures composed of extra virgin olive oil and ROO (— 0.882%, RD = 1.1891 and — 6718%, RD = 1.1275, a), ROPO (— 0.834% RD = 1.1829 and — 7.224%, RD = 1.1159, b), SO (— 0.787% RD = 1.1813 and — 6.959%, RD = 1.1205, c) CO (— 1.087% RD = 1.1873 and — 7.335%, RD = 1.1396, d).

tal geometry point of view, the fractal dimension is a measure of complexity which is used to describe the irregular nature of lines, curves, planes or volumes.

In this work, the regularization dimension (RD) and the box dimension (BD) using the plain box method have been computed by Fraclab version 2.0 (Toolbox of Matlab version 7.01.24704, R14). Considering the original signal as fractal, its graph will have an infinite length. Taking into account RD and that all regularized versions have a finite length, the RD measures the speed at which this convergence to the infinite takes place. To calculate BD, the software works in exactly the same way as when computing the regularization dimension except that in this case different box sizes are tested. In almost all cases, the estimation of fractal dimension by the box method is less accurate than the calculation by the regularization method. All necessary parameter values to calculate RD and BD were selected by default configuration settings of the software used [33].

2.3. Learning, verification and validation sample

Every dataset of the learning and verification samples is composed of seventeen aforementioned chaotic parameters (a Lyapunov exponent, 14 autocorrelation parameters, and two fractal dimensions) with their respective concentration of low grade oil in percentage (ROO, ROPO, SO or CO). Experimentally, for every adulterant oil (ROO, ROPO, CO or SO oils), 22 different concentrations of adulterating oils have been homogenously distributed from 0% (EVOO pure) to 10%. Every sample has been made three times and each sample has been UV–vis scanned three times. These parameters were calculated from the UV–vis scans from all binary mixtures composed of EVOO and ROO, ROPO, SO or CO. As an example, in Fig. 1, eight UV–vis scans selected from 817 scans which composed the database used to design the linear and non linear models in this work can be seen. Although the EVOO samples adulterated with ROPO and SO are more similar, all profiles with similar concentration values are comparable. The learning and verification samples are composed of 756 datasets, which were distributed in 189 for EVOO + ROO, 189 for EVOO + ROPO, 189 for EVOO + SO and 189 for EVOO + CO. The only difference between the verification and learning samples is that the latter is composed of 80% (605 datasets) of data and the former of the remaining 20%. Taking into account that every datum of the verification sample should be interpolated within the learning range, the data were randomly distributed between both samples [34].

On the other hand, with relation to the external validation process, the above mentioned chaotic parameters have been calculated using different UV–vis scans from binary mixtures composed of EVOO and ROO (16 samples), ROPO (15 samples), SO (15 samples) or CO (15 samples). Using these chaotic parameters and their respective adulterating oil concentration, external validation samples have been made. These external validation samples present the same format as the learning and verification samples [34].

2.4. Linear models

The linear models tested in this work are considered linear in the parameters, also called statistically linear [35]. Linear and multiple linear regressions are the most widely used and known modelling methods. They have been adapted to a broad range of situations. In a multivariate case, when there is more than one independent variable, the regression line cannot be visualized in two-dimensional space. In this case, a linear equation containing all those variables can be constructed, Eq. (4):

$$y = \beta_0 + \sum_{i=1}^{n} \beta_i x_i + \varepsilon \quad (4)$$

where, y, n, β_i ($\beta_0, \beta_1, \ldots, \beta_n$), x_i ($i = 1, 2, \ldots, n$) and ε represent response variable, number of observations, parameters of the model, independent variables, and random error, respectively [36]. The error term is an unobservable random variable that represents

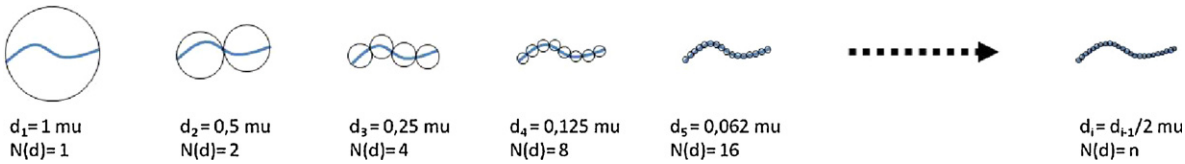

Fig. 2. Calculation procedure of fractal dimension (mu, d_n and $N(d)$ are the generic unit of distance, diameter and the number of object necessary to fill the curve, respectively).

the residual variation and will be assumed to have zero mean, constant variance and a normal distribution. The linear models are not limited to lines or planes, but include a fairly wide range of shapes [36]. In this work, the linear models and statistical analyses were carried out by SPSS version 15.0.1.

2.5. Radial basis network model

The radial basis model consists of three layers: the input, hidden radial basis and output linear, Fig. 3. The input layer has no calculation power and serves as an input distributor to the hidden radial basis layer. The input to the hidden radial basis neuron is the vector distance between its weight vector, w (self-adjustable parameter of the net), and the input vector, p, multiplied by the bias (the two last layers have biases, Fig. 3). The transfer function of radial basis neurons is a Gaussian function, Eq. (5). The radial basis function has a maximum of 1 when its input is 0. As the distance between w and p decreases, the output increases. The bias allows the sensitivity of the radial basis neuron to be adjusted. The operation of the output layer is a linear combination of the radial basis units according to Eq. (6) [37].

$$G_j(x) = \frac{1}{e^{x^2}} \tag{5}$$

$$y_k(x) = \sum_{j}^{n_h} w_{jk} \cdot G_j(x) + w_k \tag{6}$$

In Eqs. (5) and (6), y_k is the kth output unit for the input vector x, n_h is the number of hidden radial basis units, w_{jk} is the weight between the jth hidden and the kth output neurons, G_j is the notation for the output of the jth radial basis unit, and w_k is the bias.

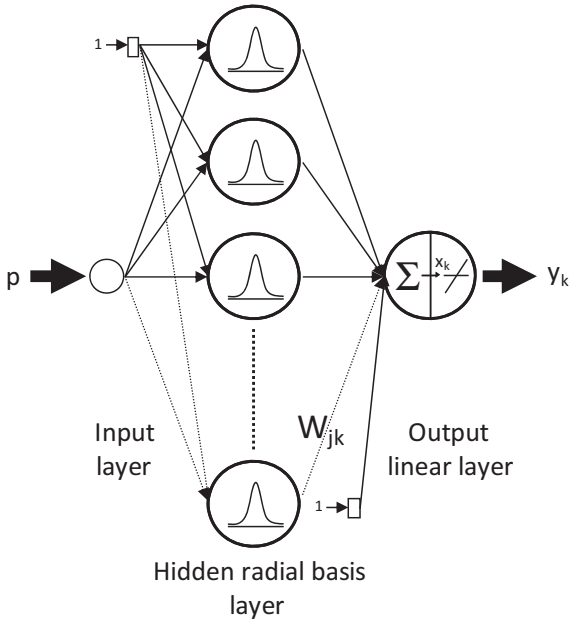

Fig. 3. Diagram of calculation of Radial basis network (đ bias node).

The type of network used here is the radial basis network exact fit. Apart from the spread constant parameter (*vide infra*), taking into account that the performance error is equal to zero, the RBN model is able to optimize all other adjustable parameters itself [37], and therefore, this type of model is simple to use. It depends on a matrix of input vectors, a matrix of target class vectors and a spread of radial basis functions (spread constant). The radial basis network algorithm provides a new exact radial basis network.

As the spread constant (SC) is the only parameter of the RBN which can be optimized, this was done by testing different spread constant values between 0.001 and 15 [37]. The response variables were the mean prediction error (MSE, %), Eq. (7), and the correlation coefficient (R^2, predicted *vs.* experimental values).

$$MSE = \frac{1}{N}\sum_{n}(r_n - y_n)^2 \tag{7}$$

In Eq. (7), N, y_n, and r_n, are the number of observations, neural network model estimation and real value, respectively. The design was analyzed taking into account that the estimations should be carried out with the need to achieve the lowest MSE and the highest values of correlation coefficient. The RBN used in this work was designed using Matlab version 7.01.24704 (R14) [37].

3. Results and discussion

A database formed by the percentage of adulterating agents ROO, ROPO, SO or CO in EVOO and the chaotic parameters (Lyapunov exponent, autocorrelation coefficients (14 parameters) and two fractal dimensions) calculated by their UV–vis scans were made. This was divided into two databases *viz.*, learning and verification samples (*vide supra*). Both linear and non linear models were optimized, verified and validated using the same learning, verification and validation databases, respectively. In this work, all statistical results shown were calculated using these two latter databases.

Firstly, the adulteration of EVOO was studied by linear models. Then, in order to improve the statistical results, a non linear model based on the RBN model has been applied. Finally, both linear and non linear models were externally validated [34].

3.1. Linear modelization of the adulteration of EVOO

To find the most suitable model to estimate the concentration of adulterating agents (dependent variable) and as a consequence of the combination of the aforementioned 17 chaotic parameters (independent variables), 262,144 models were designed. Here, six models with the best statistical results using six respective groups formed by 1 to 6 independent variables and their statistical results are shown in Table 3. As expected, the models, which use more independent variables, can better explain the response surface. Thus, the statistical results improved when more independent variables were used, Table 3. It is worth mentioning that RD is one independent variable in all proposed models to estimate the adulterating agent concentration. And a correlation coefficient value higher than 0.82 can be achieved using only this parameter.

Although the aforementioned models can be used to easily determine the adulteration of EVOO with ROO, ROPO, SO or CO,

Table 3
Estimation of adulterating agents of EVOO by linear regression models.

α_0	α_1	α_2	α_3	α_4	α_5	α_6	R^2[a]	MSE (%)[b]
116.135	−96.776 RD	–	–	–	–	–	0.827	1.273
129.128	−9.479 R_{350}	−103.376 RD	–	–	–	–	0.872	0.960
118.006	2.551 R_{50}	−7.856 R_{500}	−95.595 RD	–	–	–	0.881	0.899
120.893	−16.734 R_{100}	19.262 R_{250}	−3.987 10^6 Lia	−100.089 RD	–	–	0.897	0.788
94.335	−17.853 R_{100}	18.714 R_{250}	−3.722 10^6 Lia	−89.252 RD	15.750 BD	–	0.903	0.753
91.498	28.459 R_{250}	−11.801 R_{350}	16.733 R_{450}	−6.181 10^6 Lia	−90.647 RD	16.894 BD	0.910	0.713

[a] The [Adulterating agent] $= \sum_{i=0}^{6} \alpha_i$.

[b] Eq. (7).

in order to find the most statistically reliable model using the seventeen independent variables, the model with the best statistical results was selected. It is formed by 10 of them, Eq. (8).

$$\begin{aligned}[\text{Adulterating agent}] = {} & 83.681 + 8.482 \cdot R_{150} + 37.841 \cdot R_{250} \\ & + 18.295 \cdot R_{450} - 23.070 \cdot R_{500} \\ & + 10.322 \cdot R_{550} - 0.777 \cdot R_{600} \\ & - 4.367 \cdot R_{650} - 4.654 \times 10^6 \cdot \text{Lia} \\ & - 86.111 \cdot \text{RD} - 17.919 \cdot \text{BD} \quad (R^2 > 0.923; \\ & \text{MSE} < 0.643\%) \end{aligned} \tag{8}$$

Different combinations of all chaotic parameters presented here are suitable to quantify the ROO, ROPO, SO or CO concentrations as adulterating agents of EVOO when the former concentration is less than 10%. To sum up, linear models based on the chaotic parameters calculated by the UV–vis scans of adulterated EVOO samples can be applied to detect and quantify adulterating agents. It is noticeable that by increasing the number of independent variables of the linear models, the statistical results of the model do not improve sufficiently to justify these steps, mainly from models with six to ten independent variables. Therefore, another type of model was tested.

Better statistical results could be achieved establishing non linear models between the aforementioned chaotic parameters and adulterating agent concentrations, but the model, and so, its calculation procedure is relatively more complex. However, the poor statistical results aforementioned led us to test a non linear model which was based on radial basis network.

3.2. Non linear modelization of the adulteration of EVOO

Taking into account that a further step in the complexity of the model used has been taken, in an attempt to find the simplest non linear model, the least number of independent variables to describe the adulteration of EVOO studied has been selected. Because of this, given that the regularization dimension (fractal dimension) linearly describes the adulteration of EVOO with low cost oils studied with correlation coefficients higher than 0.82 (Table 3), the non linear model has been designed using only this independent variable. In line with this, the radial basis network model consists of only one input node (RD) and the output neuron is designed by the requirement of the model, that is, as the RBN model is designed to estimate the calculation of the adulterating agent concentration, it has one output neuron. The hidden neuron number is designed by the RBN model itself.

The only adjustable parameter of the RBN model is the spread constant (SC, *vide supra*). The SC was selected in the RBN optimisation and no experimental design was necessary. The spread constant was analysed taking into account that the estimations should be carried out using the lowest possible MSE (Eq. (7)) and highest correlation coefficient values. The optimised values for the model are shown in Table 4. Although the RBN model is more complex than the linear model, in comparison with other neural network models, the optimization of this RBN model is currently one of the most simple of all existing neural network models [37].

Table 4
Optimized parameters of RBN model and statistical results calculated by verification sample.

Parameter	Optimized value
Number of input node	1
Number of output neurons	1
Spread constant	1.3×10^{-3}
Statistical results	
Correlation coefficient	0.989
MSE (%)[a]	0.005

[a] Eq. (7).

Comparing the performance of linear and non linear models, using the verification sample, the correlation coefficient has increased from 0.92 to 0.99, respectively, but in the case of MSE the improvement is even higher, from 0.64% to 0.005%, Eq. (8) and Table 4, respectively. In principle, these statistical results are relatively good, but to guarantee the linear and non linear models as suitable to estimate the concentrations of adulterating agent concentrations, these models require to be externally validated [34].

3.3. External validation of the linear and non linear models

To validate the linear model described by equation 8 and the RBN model, a new database have been used (*vide supra*). It consists of chaotic parameters calculated by 61 datasets (10% of the number of UV–vis scans used in the learning sample), which consist of UV–vis scans from new samples constituted by EVOO and ROO, ROPO, SO or CO oils with concentrations ranging between 0% and 10% [34].

As can be seen in Fig. 4, the adulteration of EVOO with ROO, ROPO, SO or CO oils can be more adequately detected using the RBN model than by the linear model (equation 8). In particular, the correlation coefficient improves from 0.710 for the linear model to 0.966 in the RBN model. The MSE from linear to RBN models decreases by nearly twenty times, Table 5. In the light of these

Table 5
Statistical results of the external validation processes of linear and RBN models.

	Linear models	RBN model
Correlation coefficient	0.710	0.966
MSE (%)[a]	1.005	0.051

[a] Eq. (7).

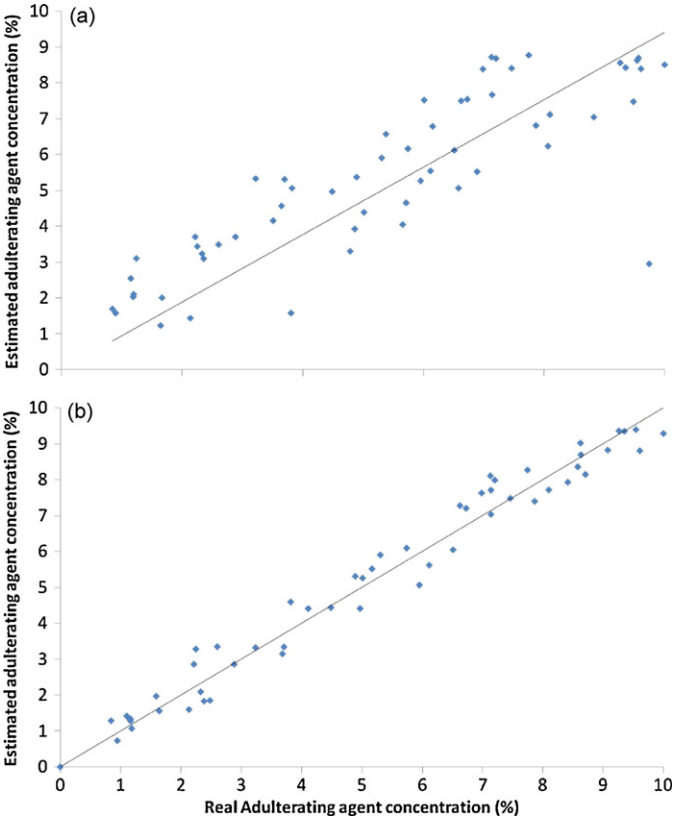

Fig. 4. External validation of linear (a, Eq. (6)) and RBN (b) models.

results, the RBN model is a reliable tool when detection of ROO, ROPO, SO or CO concentrations of less than 10% is required. Therefore, it is suitable not only to detect adulterations, but also to measure impurities when, for instance, high grade olive oil is transferred to other storage tanks which had contained lower grade olive oils and had not been adequately cleaned. In addition, given the characteristics of the analytical technique used, this detector can be applied to detect adulterations in the industrial chain of production of extra virgin olive oil.

In the light of the statistical results, the regularization dimension, which can be calculated easily, extracts the major part of the essential information from huge databases such as UV–vis scans of adulterated EVOO. In addition, the detection of the presence of other low cost and edible oils can be successfully carried out only by this parameter and RBN model. This is a promising result which could take us closer to reaching the utopia of the ideal detector of adulterations of extra virgin olive oil.

Nevertheless, taking the statistical results shown in this work into account, depending on the final application of the models, both models could be used. For faster computation, a linear model described by equation 8 could be designed and applied using experimental data to estimate with less accuracy the adulterating agents concentrations of EVOO. Otherwise, if the mathematical complexity of the model is not important or high accuracy is necessary, RBN models should be adequate.

Acknowledgements

The authors thank Claudia Mignon and Carlos Calvo for their contribution in this work and are grateful to the Spanish "Comunidad Autonoma de Madrid" for financial support of project S2009/PPQ-1545.

References

[1] J.S. Torrecilla, The Olive-its Processing and Waste Management, Nova Publishers, New York, 2010.
[2] D.S. Lee, B.S. Noh, S.Y. Bae, K. Kim, Anal. Chim. Acta 358 (1998) 163.
[3] S. Mildner-Szkudlarz, H.H. Jelen, Food Chem. 110 (2008) 751.
[4] M.J. Lerma-García, J.M. Herrero-Martínez, G. Ramis-Ramos, E.F. Simó-Alfonso, Food Chem. 107 (2008) 1307.
[5] A. Sayago, D.L. García-González, M.T. Morales, R. Aparicio, J. Agric. Food Chem. 55 (2007) 2068.
[6] M. Angiuli, C. Ferrari, L. Lepori, E. Matteoli, G. Salvetti, E. Tombari, A. Banti, N. Minnaja, J. Therm. Anal. Calorim. 84 (2006) 105.
[7] F. Marini, A.L. Magrì, R. Bucci, A.D. Magrì, Anal. Chim. Acta 599 (2007) 232.
[8] J.S. Torrecilla, E. Rojo, M. Oliet, J.C. Domínguez, F. Rodríguez, J. Agric. Food Chem. 57 (2009) 2763.
[9] V.G. Dourtoglou, T. Dourtoglou, A. Antonopoulos, E. Stefanou, S. Lalas, C. Poulos, J. Am. Oil Chem. Soc. 80 (2003) 203.
[10] R. Aparicio, R. Aparicio-Ruíz, J. Chromatogr. A 881 (2000) 93.
[11] M. Hajimahmoodi, Y. Vander Heyden, N. Sadeghi, B. Jannat, M.R. Oveisi, S. Shahbazian, Talanta 66 (2005) 1108.
[12] A. Saba, F. Mazzini, A. Raffaelli, A. Mattei, P. Salvadori, J. Agric. Food Chem. 53 (2005) 4867.
[13] S.A. Damirchi, G.P. Savage, P.C. Dutta, J. Am. Oil Chem. Soc. 82 (2005) 717.
[14] J.E. Spangenberg, N. Ogrinc, J. Agric. Food Chem. 49 (2001) 1534.
[15] E. Christopoulou, M. Lazaraki, M. Komaitis, K. Kaselimis, Food Chem. 84 (2004) 463.
[16] D. Zabaras, M.H. Gordon, Food Chem. 84 (2004) 475.
[17] M.H. Gordon, C. Covell, N. Kirsch, J. Am. Oil Chem. Soc. 78 (2001) 621.
[18] G. Fragaki, A. Spyros, G. Siragakis, E. Salivaras, P. Dais, J. Agric. Food Chem. 53 (2005) 2810.
[19] G. Vigli, A. Philippidis, A. Spyros, P. Dais, J. Agric. Food Chem. 51 (2003) 5715.
[20] T. Mavromoustakos, M. Zervou, G. Bonas, A. Kolocouris, P. Petrakis, J. Am. Oil Chem. Soc. 77 (2000) 405.
[21] R.M. Maggio, T.S. Kaufman, M. Del Carlo, L. Cerretani, A. Bendini, A. Cichelli, D. Compagnone, Food Chem. 114 (2009) 1549.
[22] E. Chiavaro, M.T. Rodriguez Estrada, C. Barnaba, E. Vittadini, L. Cerretani, A. Bendini, Anal. Chim. Acta 625 (2008) 215.
[23] E. Chiavaro, E. Vittadini, M.T. Rodriguez-Estrada, L. Cerretani, L. Capelli, A. Bendini, J. Food Lipids 16 (2009) 227.
[24] M. Jafari, M. Kadivar, J. Keramat, J. Am. Oil Chem. Soc. 86 (2009) 103.
[25] R.M. Maggio, L. Cerretani, E. Chiavaro, T.S. Kaufman, A. Bendini, Food Control 21 (2010) 890.
[26] J.S. Torrecilla, E. Rojo, J.C. Domínguez, F. Rodríguez, J. Agric. Food Chem. 58 (2010) 1679.
[27] J.S. Torrecilla, E. Rojo, J.C. Domínguez, F. Rodríguez, Talanta 79 (2009) 665.
[28] J.C. Sprott, Chaos and Time-series Analysis, Oxford University Press Inc., New York, 2003.
[29] R.L. Devaney, A First Course in Chaotic Systems, Theory and Experiment, Addison-Wesley Publishing Company, Inc., Canada, 1995.
[30] D.V. Vayenas, S. Pavlou, Ecol. Model. 136 (2001) 285.
[31] P.G. Drazin, Nonlinear Systems, Cambridge University Press, Cambridge, United Kingdom, 1992.
[32] H. Kant, T. Schreiber, Nonlinear Timer Series Analysis, Cambridge University Press, Cambridge, 2005.
[33] J.L. Véhel, Retrieved August 18, 2009. http://complex.futurs.inria.fr/FracLab/manual.html.
[34] Guidance Document on the Validation of (Quantitative) Structure Activity Relationship [(Q)SAR] Models, No. 69, OECD, Series on Testing and Assessment, Organisation of Economic Cooperation and Development, Paris, France, 2007.
[35] NIST/SEMATECH e-Handbook of Statistical Methods. Retrieved August 18, 2009, http://www.itl.nist.gov/div898/handbook.
[36] J.S. Torrecilla, J. Palomar, J. García, E. Rojo, F. Rodríguez, Chemom. Intell. Lab. Syst. 93 (2008) 149.
[37] H.B. Demuth, M. Beale, M.T. Hagan, Neural Network Toolbox for Use with MATLAB User's Guide. Version 5. Ninth printing Revised for Version 5.1 (Release 2007b), 2007.